NATIONAL ADVISORY COMMITTEE FOR AERONAUTICS

TECHNICAL NOTE 3171

SOME NEW DRAG DATA ON THE NACA RM-10 MISSILE AND A CORRELATION OF THE EXISTING DRAG MEASUREMENTS AT M = 1.6 AND 3.0

By Robert J. Carros and Carlton S. James

Ames Aeronautical Laboratory
Moffett Field, Calif.

Washington
June 1954

H

NATIONAL ADVISORY COMMITTEE FOR AERONAUTI

TECHNICAL NOTE 3171

SOME NEW DRAG DATA ON THE NACA RM-10 MISSILE AND A CORRELATION OF THE EXISTING DRAG MEASUREMENTS AT M = 1.6 AND 3.0

By Robert J. Carros and Carlton S. James

SUMMARY

The total zero-lift drag of a fin-stabilized parabolic body of revolution designated the RM-10 was investigated using 1/48-scale models launched from a gun through still air at Mach numbers near 1.6 and 3.0 and corresponding Reynolds numbers of 3.0 million and 5.0 million. Results of the present test showed that the location of transition had an important effect on the drag of this configuration. It is shown that the drag measurements of this investigation and those from other facilities can be correlated when, in addition to Mach number and Reynolds number, the effects of transition location and wall-to-free-stream temperature ratio on skin friction are taken into account.

INTRODUCTION

In 1948, at the suggestion of the Research and Development Board, the NACA undertook a special program for the evaluation of "scale effect" by means of comparative wind-tunnel and free-flight investigations on a specific model. Tests were to be conducted over a wide range of Reynolds number and of model size, and were to include measurements of total drag, pressure distribution, and location of transition where feasible. The model which was chosen for testing is a slender fin-stabilized body of revolution designated as the RM-10.

Since the inception of this coordinated program of which the present investigation is a part, tests have been conducted in six of the NACA facilities on models as small as 3 inches in length and as large as 12 feet in length (full scale), and at Reynolds numbers ranging from less than 1 million to more than 200 million. The approximate Mach number range covered has been from 0.9 to 3.3, with the majority of the data being obtained at Mach numbers near 1.6.

The details of the present investigation are described herein. A brief description of each of the other five facilities and of the corresponding models and test conditions will be found in reference 1.

Much of the information presented herein has been gathered from the works of several investigators of the NACA staff and has been in large measure summarized in reference 1.

It is the purpose of the present report, first, to present results of some recent free-flight measurements of the zero-lift drag of the RM-10 and, second, to attempt a correlation of the drag results obtained in the various facilities on the basis of four parameters: Mach number, Reynolds number, transition location, and wall-to-free-stream temperature ratio. The test Mach number of 1.6 was chosen for this investigation because this was the condition most common to previous investigations and for which the greatest quantity of drag data is available for comparison. Additional measurements were made at $M = 3$ in order to determine the possible effects of Mach number on the correlation.

These tests were conducted in the Ames supersonic free-flight wind tunnel.

SYMBOLS

A	maximum cross-sectional area of body, sq ft
C_D	total drag coefficient, $\frac{\text{total drag force}}{qA}$
$C_{D_{\alpha=0}}$	total zero-lift-drag coefficient
C_{D_c}	component drag coefficient
ΔC_D	drag increment due to angle of attack
C_L	lift coefficient
C_{L_α}	initial lift-curve slope, $\left(\frac{dC_L}{d\alpha}\right)_{\alpha=0}$, per radian
l	body length, ft
M	Mach number
q	free-stream dynamic pressure, lb/sq ft
R	Reynolds number based on free-stream properties and body length
R_T	transition Reynolds number based on free-stream properties and length of run of the laminar boundary layer
r	radius of body cross section, ft
T_w	temperature of model surface, deg Rankine

T_∞ free-stream static temperature, deg Rankine

t time, sec

x axial distance from body nose, ft

x_T axial distance from body nose to location of transition, ft

$\bar{\alpha}$ average angle of attack, radians

MODELS AND TEST CONDITIONS

For this investigation small-scale test models were launched from a gun in the diffuser of the 1- by 2-foot Ames supersonic free-flight wind tunnel. (To achieve the Mach numbers of this test, no air flow through the tunnel was necessary.) The models flew through still air in the test section where a photographic record of the time-distance-attitude history of a portion of each model flight was obtained. From this record, total drag was obtained for a number of test conditions in which Mach number, Reynolds number, and transition location were treated as independent variables, and skin temperature was invariant. The test facility and technique are described in detail in reference 2.

Models

The RM-10 is a parabolic body of revolution having cruciform swept fins attached near the base. Figure 1 is a drawing of the model showing the geometry and giving the equation of the curve which defines the body profile. Figure 2 is a photograph of a model. The scale of the model for this investigation (1/48) was chosen to permit the model to be fired from a 20 mm smoothbore gun. Although most of the model bodies were turned from 75 S-T aluminum, a few were made of magnesium alloy and hollowed out to reduce their mass and hence increase their deceleration in the test section. All fins were made of 75 S-T aluminum and were pinned into slots in the bodies. Each model, after assembly, was examined under magnification for conformity with the specified dimensions. The body tip was hand polished to produce a smooth symmetrical profile. This operation resulted in a tip radius averaging about 0.2 percent of the maximum body diameter, and shortened the body by about 0.5 percent of its length.

Test Conditions

Seventeen test models were fired at nominal Mach numbers of 1.6 and 3.0 through still air in the test section. For most of the models, the nominal Reynolds numbers were 3×10^6 and 5×10^6, respectively. For four of the rounds at $M = 1.6$, the Reynolds number was approximately doubled by pressurizing the test section. The skin temperature of the models remained essentially constant and equal to free-stream static temperature due to the extremely short duration of flight.

Boundary-layer trips were used on several of the models in order to establish transition at predetermined locations along the body. A number of trips were tried, many of which were not effective in producing turbulence. The weakest trip which caused immediate transition was a fine screw thread turned on the body at the place where transition was desired. Figure 3 is a photomicrograph of a typical trip placed near the body nose. Pertinent dimensions are superimposed on the photograph.

The test conditions for all rounds are summarized in table I.

DATA REDUCTION AND PRECISION

From the photographic record of the history of each model flight the zero-lift-drag coefficient and transition location were obtained.

Drag Coefficient

The deceleration of each model was calculated from the time-distance data and combined with the known mass of the model to give the drag force, which was then converted to coefficient form. The reader is referred to reference 2 for a detailed discussion of this method of data reduction.

Angle-of-attack correction.- In launching the models, small, unavoidable, pitching oscillations were induced which in turn produced small increments of drag due to angle of attack. These increments were of the order of 5 percent of the total drag. To obtain the zero-lift-drag coefficients from the measured data, it was necessary to account for these drag increments. This was done for each round by subtracting the drag increment from the measured drag coefficient according to the relation:

$$C_{D_{\alpha=0}} = C_D - \Delta C_D \qquad (1)$$

in which ΔC_D, the drag increment due to pitching, is a function of the mean square of the angle of attack $\overline{\alpha^2}$. The value of $\overline{\alpha^2}$ was determined

for each round from the angle-of-attack history of the observed portion of flight by integrating the time variation of α^2. Then ΔC_D was calculated from the equation:

$$\Delta C_D = C_{L_\alpha} \overline{\alpha^2} \tag{2}$$

Within the angle-of-attack range to which it is applied here (0° to 3°, approximately), equation (2) is well supported by the experiment of the 1- by 3-foot tunnel staff, but not by the results of the 8- by 6-foot and 9-inch tunnel experiments despite the fact that all three experiments, under widely differing test conditions, agree closely on the value of initial lift-curve slope. Nevertheless, equation (2) appears to represent the average of the available results, all of which fall within ±25 percent of the values given by equation (2).

At Mach number 1.6 the experimental value for C_{L_α} of 11 per radian was used (1- by 3-foot tunnel). At $M = 3$ where no experimental data are available, this value was reduced, using as a guide the theoretical variation of C_{L_α} with Mach number for wings given by Piland (ref. 3). The resulting value of C_{L_α} was 7.5 per radian.

For a round having the average angle-of-attack correction of 5 percent, the error in $C_{D_{\alpha=0}}$, after the correction has been made, should be within 25 percent of the correction, or approximately ±1.5 percent of $C_{D_{\alpha=0}}$. To indicate the magnitude of these angle-of-attack corrections, the values of $\overline{\alpha}$ and the ratio $\Delta C_D/C_{D_{\alpha=0}}$ for each round are listed in table I.

Trip-drag correction.- The type of boundary-layer trip used with each round is indicated in table I. A very rough estimate of the drag due to the boundary-layer trip used on round number 1 was obtained assuming each particle of carborundum to be a sphere and giving it a drag coefficient of 1 based on its own frontal area. This calculation gave a trip drag coefficient equal to approximately 2 percent of C_D. The measured value of C_D was therefore reduced by this amount. An equal correction was made for the drag of the trip used on round number 2 which was believed to be of the same order of magnitude as that on round number 1.

No correction was applied to the data from models having the screw-thread trip. Unpublished results of some tests made at this facility on hollow cylinders using this trip show for that application that the drag increment due to the presence of the trip was negligible.

Transition Location

Transition location was determined by observation of the shadowgraphs. Two criteria were used: first, the development of eddies in

the boundary layer which appear to disrupt the heavy diffraction line usually clearly defined with a laminar boundary layer; and second, the turbulent appearance of the flow field adjacent to a turbulent boundary layer. These criteria are applied simultaneously in making each observation. The authors are unable to present a suitable photographic example of a transitional boundary layer because the definition in the transition region, while adequate in the original shadowgraph, suffers excessively in reproduction. However, figures 4(a) and 4(b) are shadowgraphs of models having fully laminar and fully turbulent flow, respectively.

Tests at this facility and others have shown that the position of natural transition is time dependent and also depends on meridian position[1] and angle of attack. The usual variation of natural transition on a given round due to these causes was about 0.30l. For this reason, many observations of x_T were made from which a statistical average was obtained. Seven shadowgraphs of each model flight provided a total of 14 readings since each side of the model profile was treated independently of the opposite side. Three of the shadowgraphs were obtained in a plane normal to that of the other four. This was considered to be a sample sufficient to result in a reasonably good average value of R_T.

From considerations of the variation of transition location, its definition in the shadowgraphs, and of the repeatability of readings by different individuals, the uncertainty in R_T/R is believed to be ±8 percent in the worst case and ±3 percent on the average.

Precision

In the preceding paragraphs, errors in the test results due to making the drag correction for angle of attack and in determining transition location have been discussed. Other sources of error not already discussed include the systematic and random errors of measurement, small variations in model dimensions, and possible differences between visible transition and its true position. The possible magnitudes of these errors have been carefully considered and are believed to be small. It is estimated that the over-all accuracy of the drag data, after corrections, is within ±3 percent. Mach number and Reynolds number are estimated to be accurate to within ±0.5 percent and ±1 percent, respectively.

RESULTS AND DISCUSSION

The experimental results of zero-lift-drag coefficient, $C_{D_{\alpha=0}}$, versus Mach number from the present test and from other facilities are

[1]An excellent portrayal of this phenomenon is given in a series of luminous lacquer photographs presented by Potter in figures 16-20 of reference 4.

plotted in figure 5.[2] The Reynolds number varies from 2.7 million to 140 million at Mach numbers near 1.6, and from 5 million to 134 million at Mach numbers near 3.0. The variation between the minimum and maximum values of drag coefficient at $M = 1.6$ amounts to more than 40 percent of the mean. The same observation is true of the data at $M = 3$. It is evident, therefore, that for a missile of this type some variables other than Mach number need be considered to correlate the data.

The viscous drag of this configuration comprises approximately 30 percent of the total drag for laminar flow and approximately 50 percent of the total drag for turbulent flow and, therefore, Reynolds number would be expected to be an important variable. Accordingly, the data of figure 5 are replotted against Reynolds number in figures 6(a) and 7(a). Small adjustments based on the slope of the $C_{D_{\alpha=0}}$ versus Mach number curve[3] were applied to the data so that in each figure a comparison could be made at a common Mach number. To provide a reference framework, curves of the predicted variation of C_D with R are placed in the figures. These curves were obtained by summing the estimated variation with Reynolds number of the skin-friction drag and the body base drag. A discussion of the methods used to obtain these estimates will be found in the Appendix and the component drag curves will be found in figures 6(b) and 7(b). Since only the variation with Reynolds number and not the absolute value of the total drag coefficient was calculated, the curves for the turbulent-boundary-layer case have been drawn to pass through that data of the present investigation for which the body boundary layer was known to be completely turbulent.[4] At Mach number 1.6 (fig. 6(a)), the curve of the predicted variation for laminar flow is drawn at the theoretical displacement from the turbulent curve. At Mach number 3, the predicted variation for laminar-boundary-layer flow was drawn through the laminar data of the present investigation rather than being displaced the theoretical distance from the turbulent curve. This positioning was arbitrarily applied because of inability to predict the absolute magnitudes of base drag, hence curve separation, at this Mach number (see Appendix).

---

[2]Some of the PARD data presented in this report were obtained through recent correspondence with that facility.

[3]Figure 13 of reference 1 was used to determine the value of dC_D/dM. Figure 5 of the present report gives the same value (0.04) if the mean slope is used.

[4]An estimate of the total drag coefficient for turbulent flow, based on a summation of the wave and friction drag of the body and fins, plus the body base drag falls about 10 percent below the experimental value at a Reynolds number of 6 million. The difference is probably due, in large part at least, to the influence of the fin pressure field on the body base pressure, which effect was not accounted for in the total drag estimate.

Figures 6(a) and 7(a) indicate a partial correlation of the data on the basis of Reynolds number in that the data for turbulent flow tend to be associated with the turbulent curve and the data for laminar flow tend to be associated with the laminar curve, while those data for which the flow was transitional scatter for the most part between the curves. At M = 3 the correlation on the basis of Reynolds number is inconclusive for lack of data, although it appears that the theory does not fit the existing data as well at this Mach number as at M = 1.6. In figure 6(a) the two fully turbulent points from the 4- by 4-foot tunnel which fall below the turbulent curve were obtained using a model supported on a wire which was coincident with the axis of symmetry of the model. An effectively higher Reynolds number of the boundary layer was thus caused to exist because of the initial thickness which the boundary layer possessed at the body nose. Movement of these points in the direction of higher Reynolds number would improve the agreement with the other turbulent data.

Conditions other than Mach number and Reynolds number which varied widely among the various experimental investigations are those of heat transfer and transition location. These two parameters were next considered to determine their effects on the correlation of the drag data. Rather large differences in the ratio of skin temperature to free-stream static temperature existed between the test conditions of the various facilities (for the same Mach number and Reynolds number conditions), particularly between wind-tunnel and free-flight experiments. In order to put the data on a comparative basis, it was necessary to eliminate the differences in drag coefficient which might be attributed to differences in heat-transfer rate. Accordingly, this effect was taken into account at Mach number 1.6 by imposing the condition that skin temperature be equal to free-stream static temperature (the test condition of the present investigation) and adjusting all the data to this condition. For the laminar boundary layer, data were adjusted by the difference in friction coefficient obtained using appropriate constant-surface-temperature values from the theoretical work of Klunker and McLean, reference 5. The same procedure was used for the turbulent boundary layer, based on the friction calculations briefly outlined in the Appendix. The resulting data points, together with the curves of figure 6(a), are plotted in figure 8. Comparison of this figure with figure 6(a) reveals that the effect of heat-transfer differences is small at M = 1.6, although in the cases of both fully laminar and fully turbulent flow, the adjustments move the data points in such a way as to bring about better alinement of the points with each other. In comparison with the data, the theoretical curve for turbulent flow appears to be somewhat low in the high Reynolds number range. This discrepancy may indicate either that the rate of change of drag coefficient with Reynolds number for turbulent flow is somewhat overestimated by the theory or that the entire curve should be moved slightly upward. While the effect of heat-transfer rate is shown to be small at this Mach number, its importance would be expected to increase with increasing Mach number and therefore should not be overlooked when comparing data obtained under differing heat-transfer conditions.

Figures 7(a) and 8 show that a major variable affecting the drag of the RM-10 missile is the position of boundary-layer transition. Data from the present investigation indicate a drag increase of 30 percent at a Mach number of 1.6 and 50 percent at a Mach number of 3.0 due to change in flow from laminar to turbulent. Data from the Langley 4- by 4-foot supersonic wind tunnel confirm this large effect of transition position on the drag. As Reynolds number is increased, the theory indicates that the difference between the laminar and turbulent drag coefficients decreases. It is interesting to note that the PARD data show a considerable variation in drag coefficient at Reynolds numbers around 50 million. However, there is in this case no direct evidence to show that these variations were or were not due to changes in the boundary-layer condition. If the drag differences shown were due to boundary-layer condition, it would be indicative of extensive laminar flow in some of the PARD tests.

The effect of transition location will now be examined in somewhat greater detail, using data of the present investigation. These data are plotted in figure 9 as $C_{D_{\alpha=0}}$ versus the ratio of transition Reynolds number to free-stream Reynolds number, R_T/R, at a Mach number of 1.6 and a Reynolds number of 3.0 million.[5] The theoretical variation of the combined skin-friction drag and base drag coefficients with R_T/R is represented by the dash curve on this figure. The method of obtaining this variation is discussed in the Appendix. The resultant curve was positioned for the best fit of the data. The theoretical curve shows a discontinuous drop in $C_{D_{\alpha=0}}$ at an R_T/R of 1. This is due to the calculated change in base drag coefficient which results when the transition point shifts across the body base. In the real viscous flow the decrease in base drag would be expected to occur gradually over a small range of R_T/R, that is, as the transition point moves off of the body and into the wake.

There are three classes of data in figure 9. The data plotted as lines with a symbol located at the midpoint represent rounds for which no trip or an inadequate trip was used. The length of the line represents the uncertainty in locating transition. The filled symbols represent rounds for which the screw-thread trip was used. The open symbols represent rounds for which the models were polished to allow a fully laminar boundary layer. The experimental variation is reasonably well predicted by the theory except at the lowest values of R_T/R, the maximum discrepancy being about 7 percent of $C_{D_{\alpha=0}}$. The reason for the unexpected drop in $C_{D_{\alpha=0}}$ below $R_T/R = 0.35$ is not clearly understood. The foregoing discussion of figure 9 also applies to figure 10 which is a plot of $C_{D_{\alpha=0}}$ versus R_T/R for a Mach number of 3.0 and a Reynolds number of 5.0 million.

[5] The data were adjusted to a common Mach number by the method discussed previously and to a common Reynolds number by moving along lines of constant transition location, using figure 6(a).

The data from other facilities adjusted to a Mach number of 1.6, a Reynolds number of 3.0 million, and a skin temperature equal to free-stream static temperature by the methods described previously are plotted in figure 11. The experimental curve of the present test is also included in this figure for comparison purposes. When the effects of transition location and heat transfer are accounted for, the data agree well except for two data points from the 4- by 4-foot wind tunnel which may have had more laminar flow present than suspected. The body-alone data from other facilities which are also included in this figure correlate well with the theoretical curve.

CONCLUDING REMARKS

Free-flight drag data have been presented for a fin-stabilized parabolic body of revolution at Mach numbers of 1.6 and 3.0 and Reynolds numbers of 3.0 million and 5.0 million. The zero-lift total-drag data of the present investigation were found to be critically dependent upon the location of transition. The inclusion of the effects of transition position and heat transfer resulted in a considerably more systematic correlation of the data from the various facilities than could be made by considering Mach number and Reynolds number alone.

Ames Aeronautical Laboratory
National Advisory Committee for Aeronautics
Moffett Field, Calif., Feb. 10, 1954

APPENDIX

THEORETICAL METHODS USED FOR PREDICTING DRAG COMPONENTS

The three drag components believed to be most strongly affected by Reynolds number variation, namely, body friction, fin friction, and base drag, were calculated for the Reynolds number range $10^6 < R < 3 \times 10^8$.

In computing skin friction, two-dimensional coefficients were assumed to apply both on the body and on the fins. Laminar friction was computed using the method of Van Driest-Crocco (ref. 6). Turbulent friction was obtained using a set of empirical equations, which have been faired to experimental data obtained on hollow-cylinder models at several values of T_w/T_∞. These equations define the ratio of compressible friction coefficient to the incompressible coefficient as a function of Mach number and T_w/T_∞ and constitute an interpolating method for extending the experimental results over a wide range of test conditions. This method is as yet unpublished. The incompressible friction was computed from the Karman-Schoenherr equation (ref. 7).

In the calculations, the fin boundary layer, because of the relatively low Reynolds numbers and favorable chordwise pressure gradients, was assumed to be laminar over the entire Reynolds number range. On the body, the ratio R_T/R was treated as an independent variable although only the curves for fully turbulent and fully laminar flow ($R_T/R = 0, 1$, respectively) are presented in figures 6(a) and 7(a). For the general case of transitional flow (i.e., $0 < R_T/R < 1$), the above methods were used to compute the friction drag of the laminar and turbulent portions of the body boundary layer. The Reynolds number limits of the turbulent region were measured from a hypothetical origin, the location of which was determined from consideration of the rates of growth of the laminar and turbulent boundary layers and the assumption that their momentum thicknesses must be equal at the transition point.

The base drag was calculated neglecting fin-interference effects[1] (i.e., for the body alone) using the method of Chapman (ref. 8) which accounts for the influence of Mach number, Reynolds number, body shape, and type of boundary-layer flow. In making the calculations it was found that the magnitude of base pressure was sensitive to the influence

[1]Because of the complicated flow pattern in the vicinity of the fins, it was considered impractical to attempt an accurate estimate of these effects. A rough estimate was made of the effects of fin interference on the base drag using two-dimensional shock-expansion theory applied to a streamwise section of the fin. The pressures in the region of the trailing edge of the fin and behind the fin were estimated and found to be from 1 percent greater to 25 percent less than the base pressure of the body alone. It therefore appeared that the fin pressure

of body shape but that its variation with Reynolds number was not. Since this method depends upon a correlation of experimental data at a given Mach number, it is necessary to interpolate or extrapolate in order to use the method at other Mach numbers. The base-drag estimate at $M = 1.6$ was obtained by interpolation. No reliable extrapolation of the correlation could be made to obtain values for base drag at $M = 3.0$. Since the data from reference 1 indicate that in this Mach number range the effect of Mach number on base drag is small, the correlation at $M = 2.0$ of reference 8 was used to predict the variation of base drag with Reynolds number at $M = 3.0$. No attempt was made to estimate the absolute magnitude of the base drag at this Mach number. Therefore, in figure 7(b) the base drag at Reynolds number 10^6 was assigned a value of zero, and the variation from this value is plotted.

Curves similar to those of figures 6(a) and 7(a) were calculated for intermediate values of R_T/R by the method just described. Cross plots of these curves at the appropriate Reynolds numbers were then used to obtain the curves of figures 9, 10, and 11.

---

field could affect the base drag by as much as 10 percent of the total drag at $M = 1.6$.

The influence of Reynolds number in this respect should appear as small changes in the pressure distribution over the fins and as changes in fin wake thickness. It is possible that such effects of Reynolds number could account for the apparent overestimate by the theory of the slope of the C_D vs. R variation in figures 6(a) and 7(a).

REFERENCES

1. Evans, Albert J.: The Zero-Lift Drag of a Slender Body of Revolution (NACA RM-10 Research Model) as Determined from Tests in Several Wind Tunnels and in Flight at Supersonic Speeds. NACA TN 2944, 1953.

2. Seiff, Alvin, James, Carlton S., Canning, Thomas N., and Boissevain, Alfred G.: The Ames Supersonic Free-Flight Wind Tunnel. NACA RM A52A24, 1952.

3. Piland, Robert O.: Summary of the Theoretical Lift, Damping-In-Roll, and Center-Of-Pressure Characteristics of Various Wing Plan Forms at Supersonic Speeds. NACA TN 1977, 1949.

4. Potter, J. L.: New Experimental Investigations of Friction Drag and Boundary Layer Transition on Bodies of Revolution at Supersonic Speeds. NAVORD Rep. 2371, Apr. 24, 1952.

5. Klunker, E. B., and McLean, F. Edward: Effect of Thermal Properties on Laminar-Boundary-Layer Characteristics. NACA TN 2916, 1953.

6. Van Driest, E. R.: Investigation of Laminar Boundary Layer in Compressible Fluids Using the Crocco Method. NACA TN 2597, 1952.

7. Schoenherr, Karl E.: Resistance of Flat Surfaces Moving Through a Fluid. Soc. Nav. Arch. and Marine Engrs., Trans., vol. 40, 1932, p. 279.

8. Chapman, Dean R.: An Analysis of Base Pressure At Supersonic Velocities and Comparison With Experiment. NACA Rep. 1051, 1951.

TABLE I.- TABULATION OF TEST CONDITIONS

Round	Type of boundary-layer trip	Trip station, x/l	M	R, millions	$\bar{\alpha}$ deg	$\frac{\Delta C_D}{C_{D_{\alpha=0}}}$
1	6 particles of No. 100 emery equally spaced around the body	0.03	1.43	4.84	1.72	0.031
2	band of No. 180 carborundum	.013 to .072	1.55	2.76	2.39	.071
3	none	- - -	1.63	5.70	3.28	.137
4	none	- - -	1.68	2.97	2.70	.092
5	none	- - -	1.69	3.06	1.85	.037
6	screw thread	.025 to .125	1.69	5.95	2.84	.113
7	screw thread	.223 to .325	1.70	2.90	3.30	.120
8	screw thread	.600 to .700	1.70	2.92	1.84	.040
9	screw thread	.020 to .120	1.71	6.00	1.84	.042
10	none	- - -	1.73	3.00	1.00	.014
11	none	- - -	1.82	3.23	1.44	.031
12	screw thread	.016 to .075	2.96	5.27	1.37	.019
13	screw thread	.613 to .722	3.01	5.28	2.46	.077
14	none	- - -	3.01	5.35	1.28	.021
15	none	- - -	3.10	5.60	2.25	.047
16	screw thread	.016 to .125	3.11	5.51	2.32	.053
17	none	- - -	3.25	5.87	.87	.012

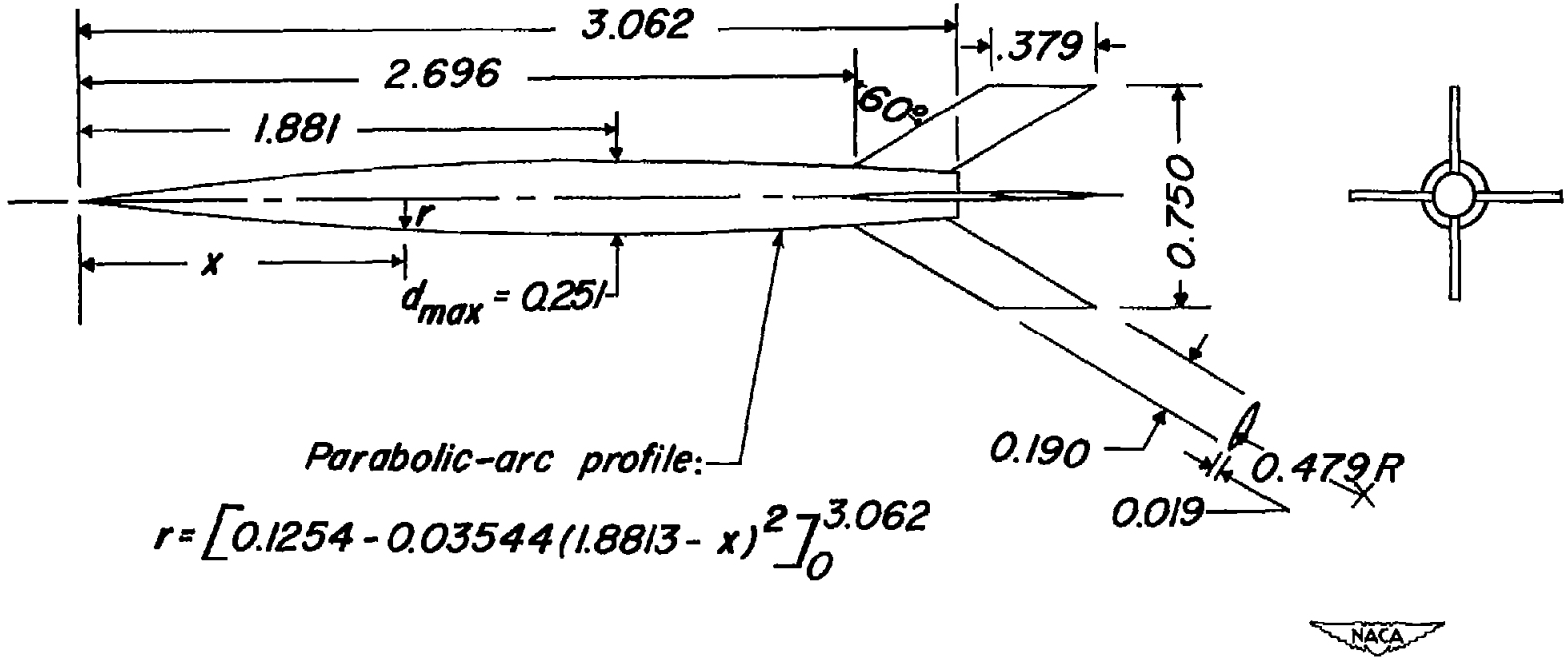

Note: All dimensions are in inches.

Figure 1.- Drawing of 1/48-scale NACA RM-10 missile.

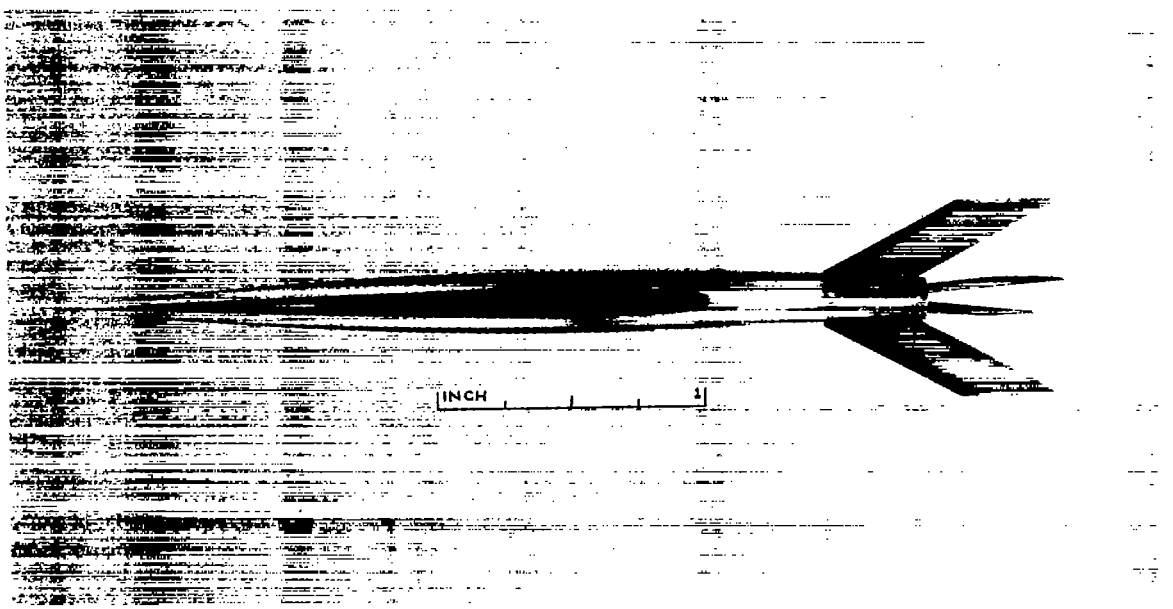

Figure 2.- Photograph of a typical RM-10 model.

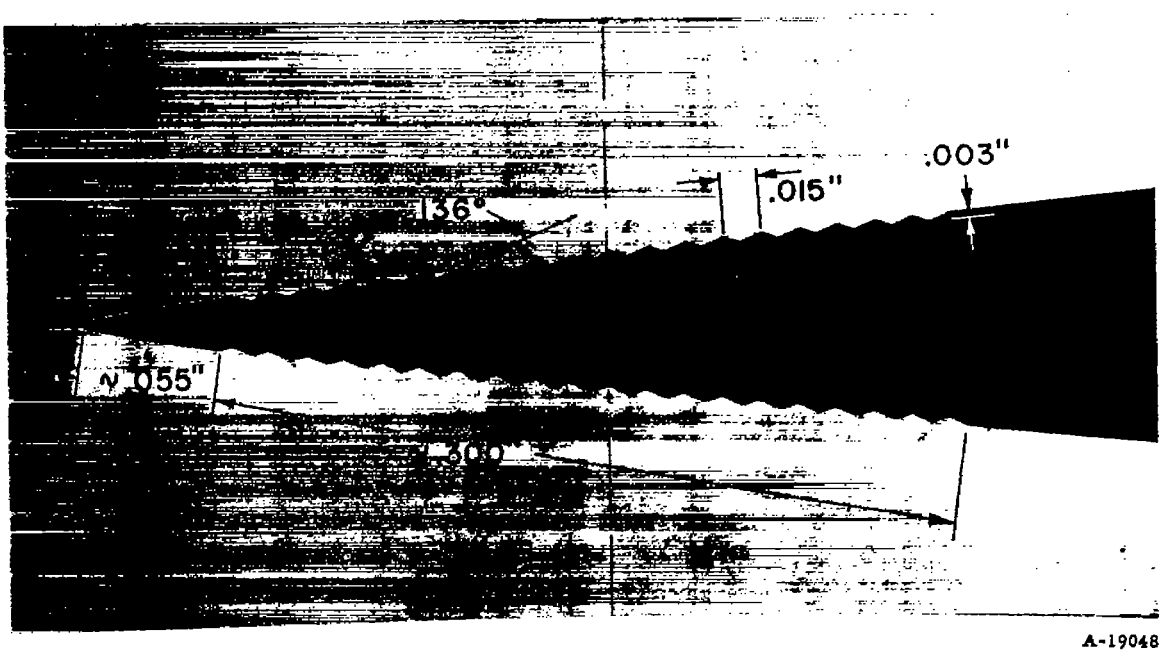

Figure 3.- Photomicrograph of a screw-thread boundary-layer trip placed at the model nose. Dimensions are shown in inches.

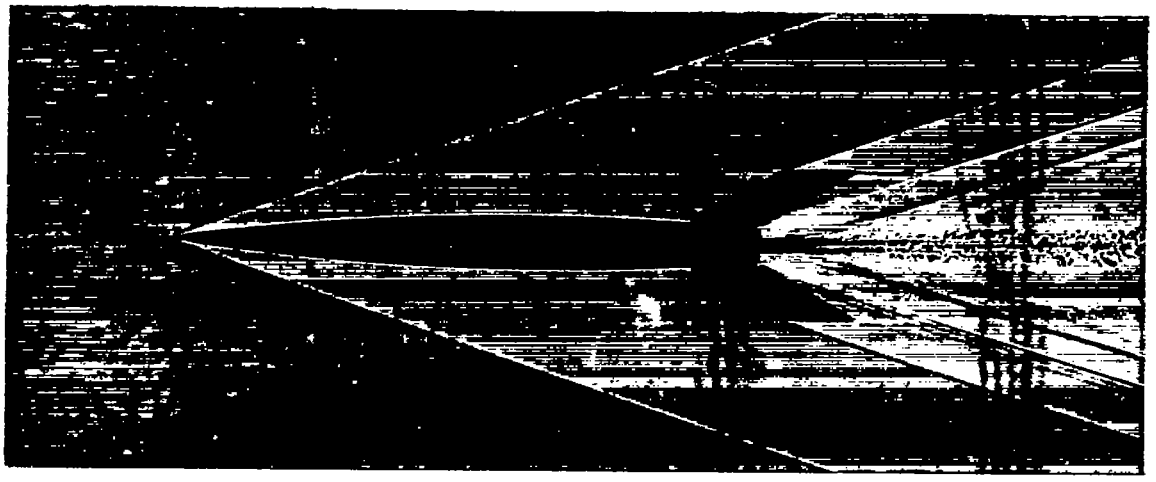

A-19049

(a) Laminar boundary layer.

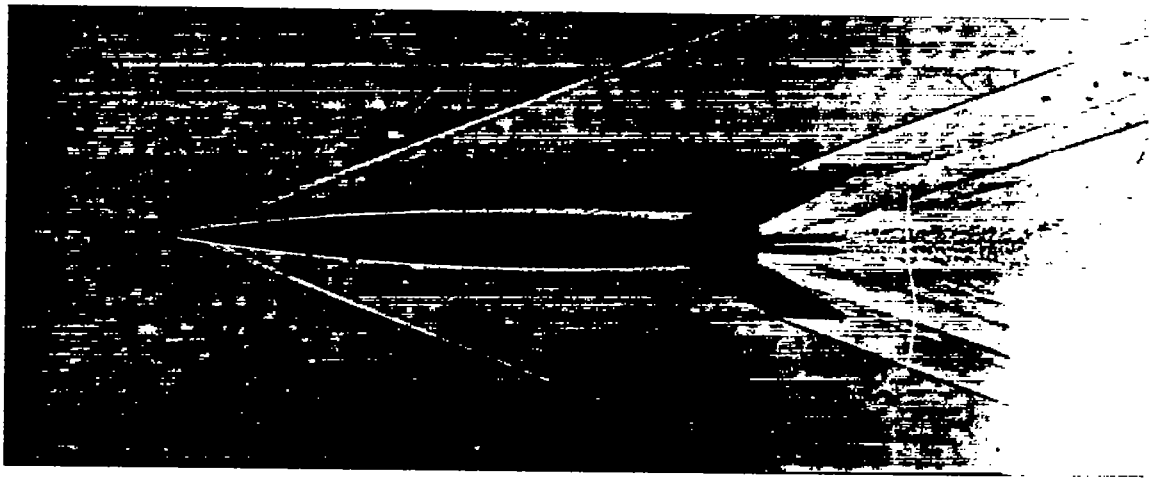

A-19050

(b) Turbulent boundary layer; trip at body nose.

Figure 4.- Shadowgraphs of typical models in flight showing examples of laminar and turbulent boundary layers ($M \approx 3$, $R \approx 5.5 \times 10^6$).

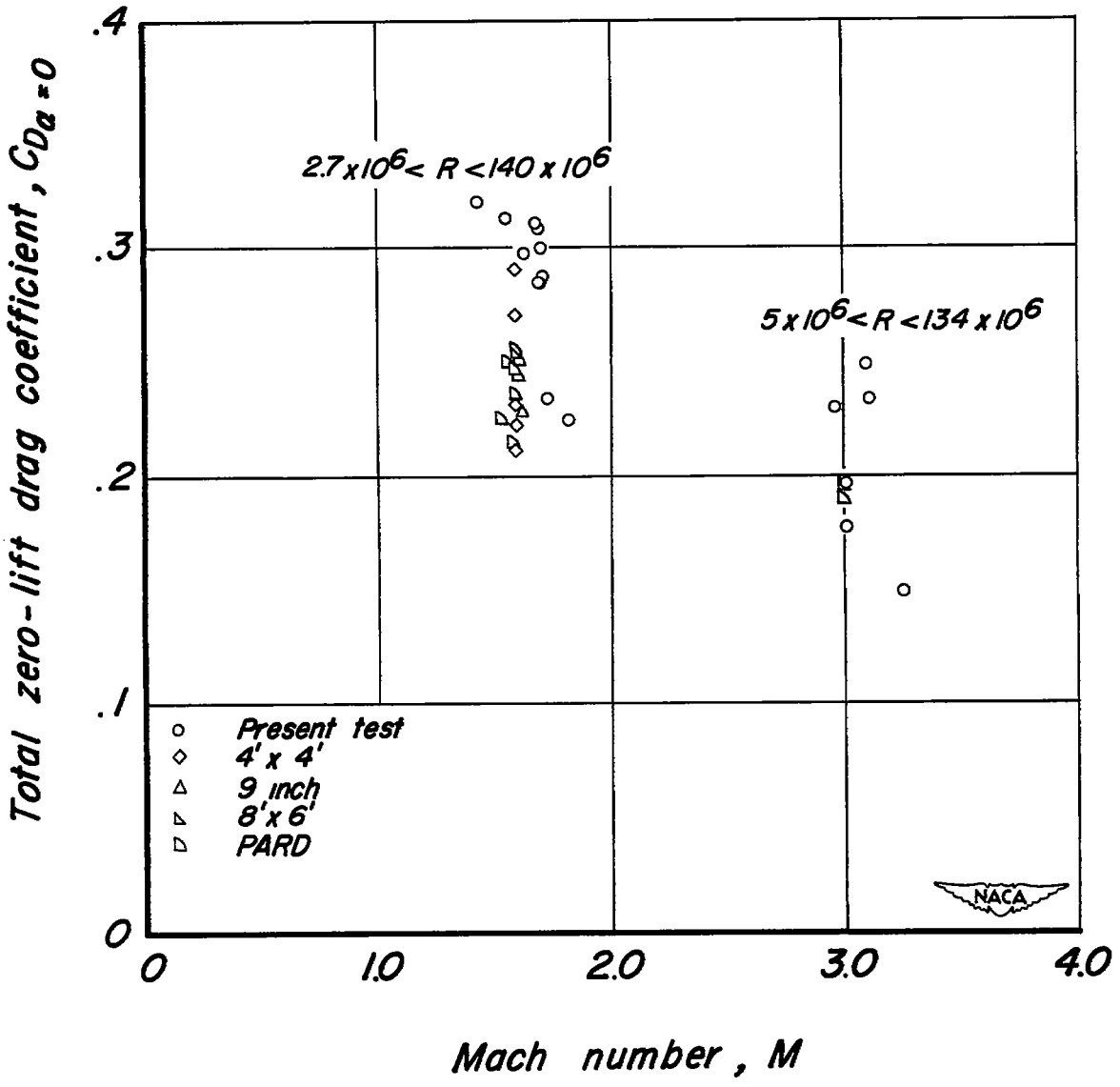

Figure 5.- Total zero-lift drag coefficient variation with Mach number.

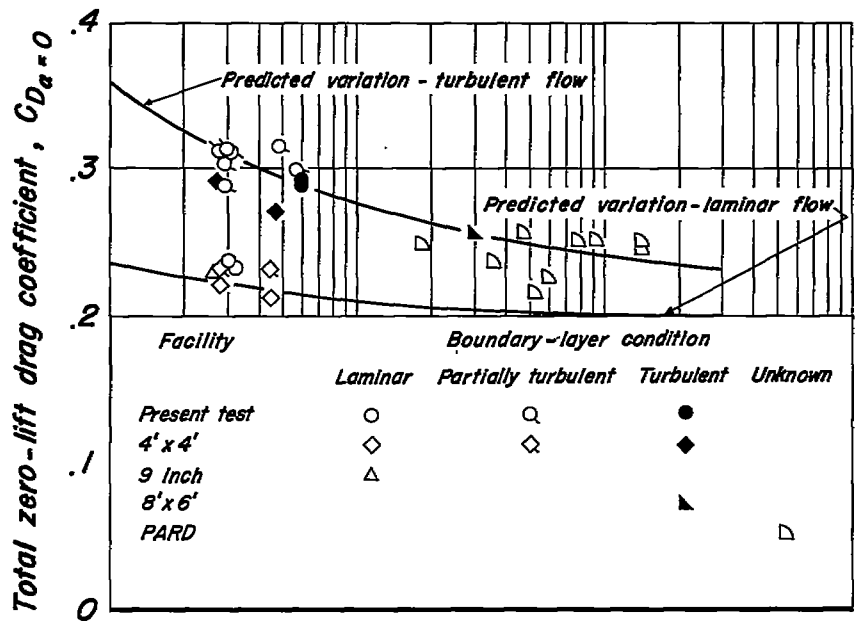

(a) Experimental results.

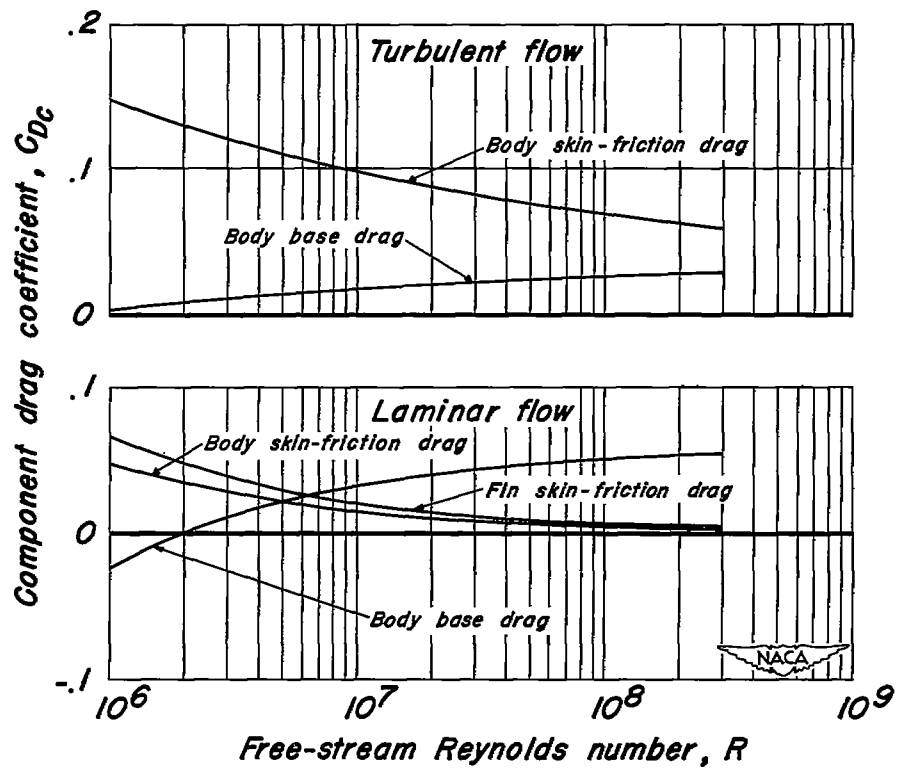

(b) Predicted variation for components.

Figure 6.- Variation with free-stream Reynolds number of the zero-lift drag coefficient at M = 1.6.

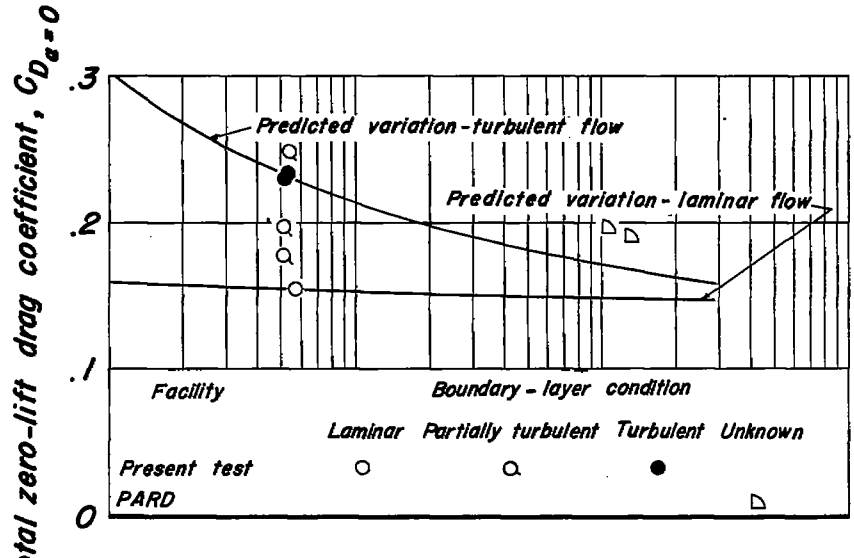

(a) Experimental results.

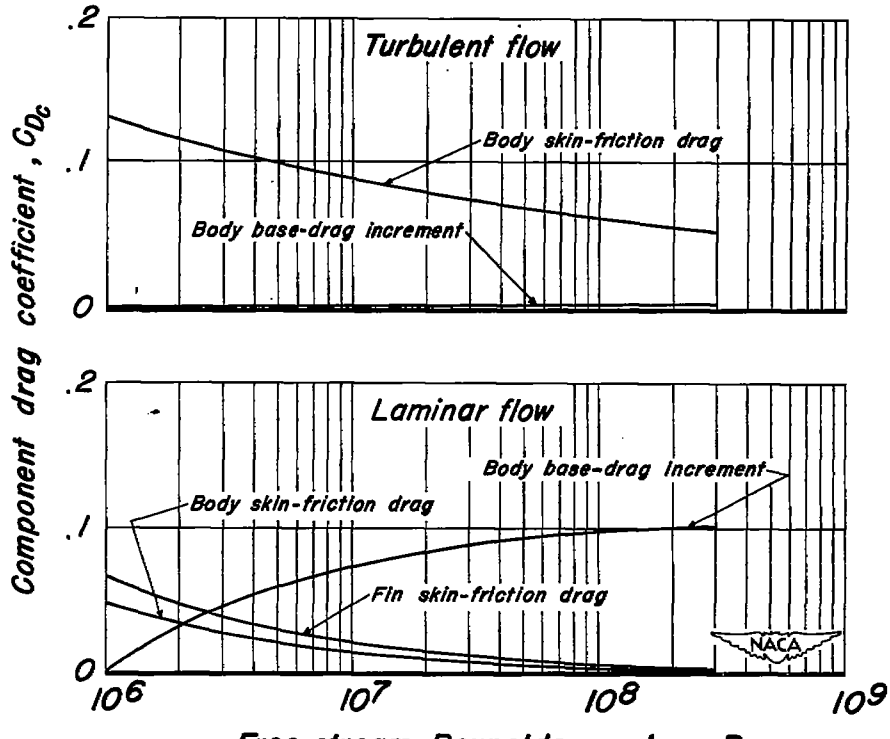

(b) Predicted variation for components.

Figure 7.- Variation with free-stream Reynolds number of the zero-lift drag coefficient at M = 3.0.

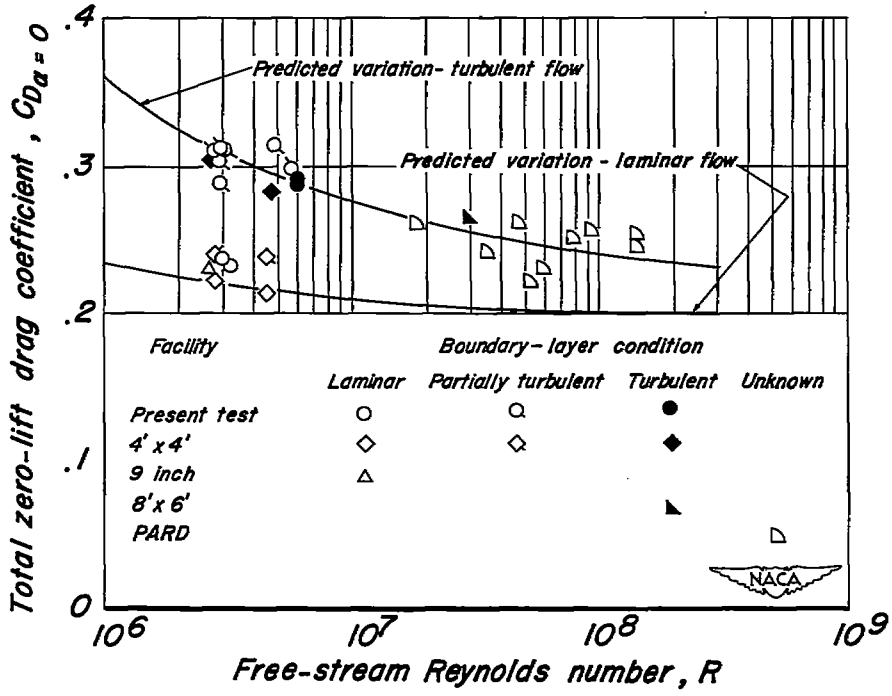

Figure 8.- Variation with free-stream Reynolds number of the total zero-lift drag coefficient at M = 1.6 (data adjusted to the condition $T_w = T_\infty$).

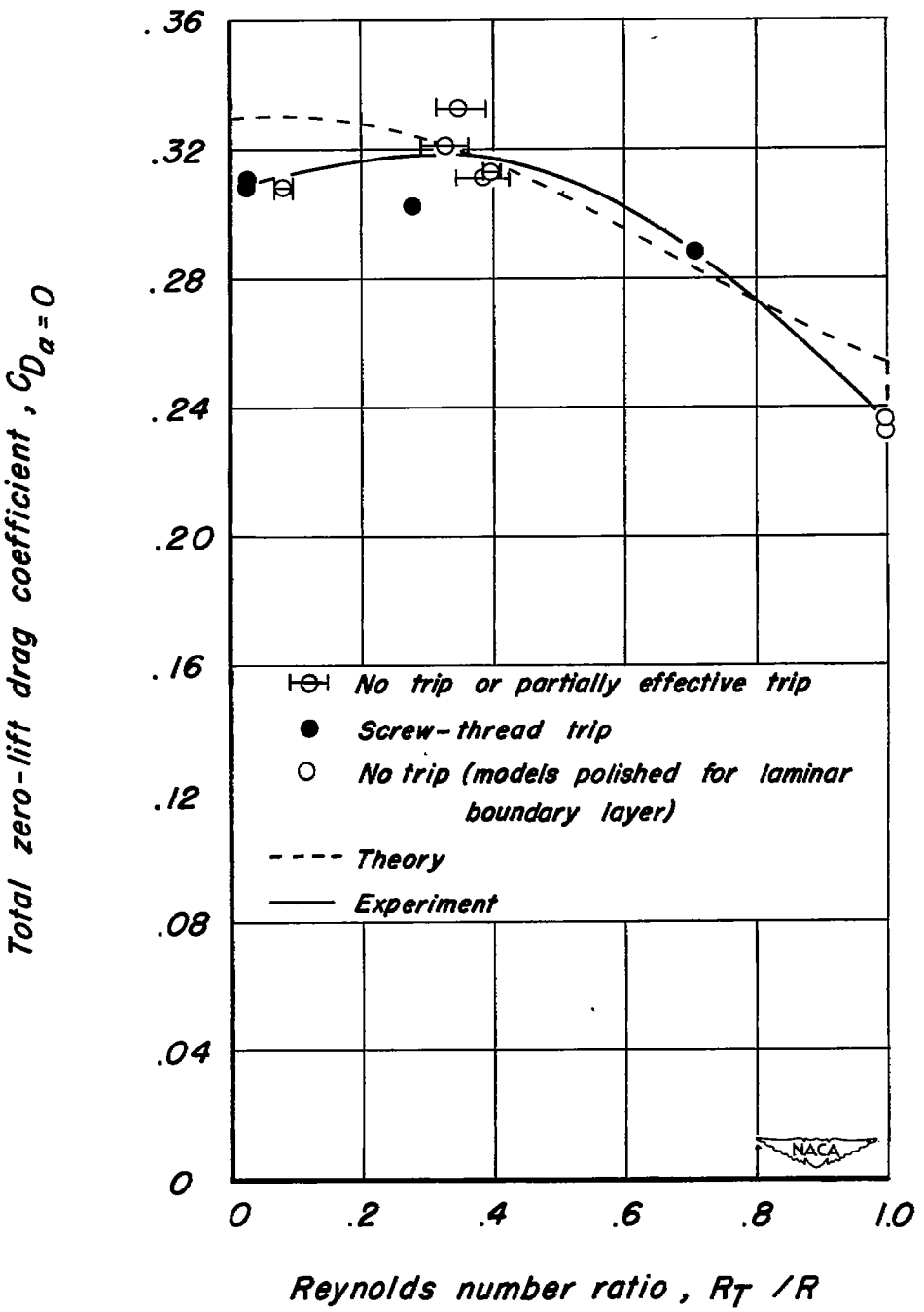

Figure 9.- Variation with transition location of the total zero-lift drag coefficient for the present test. ($M = 1.6$, $R = 3.0 \times 10^6$, $T_W = T_\infty$)

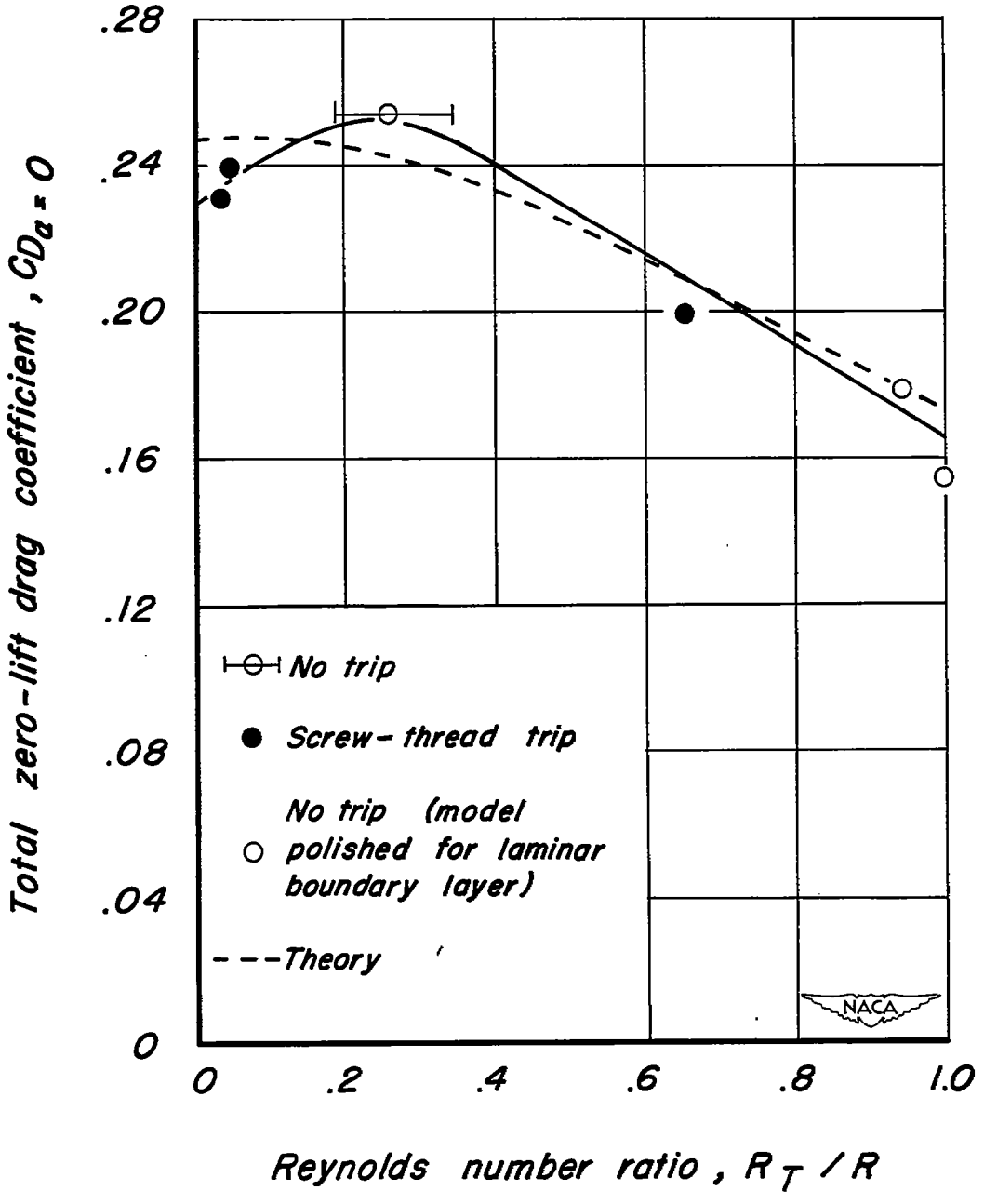

Figure 10.- Variation with transition location of the total zero-lift drag coefficient for the present test ($M = 3.0$, $R = 5.0 \times 10^6$, $T_W = T_{\infty}$).

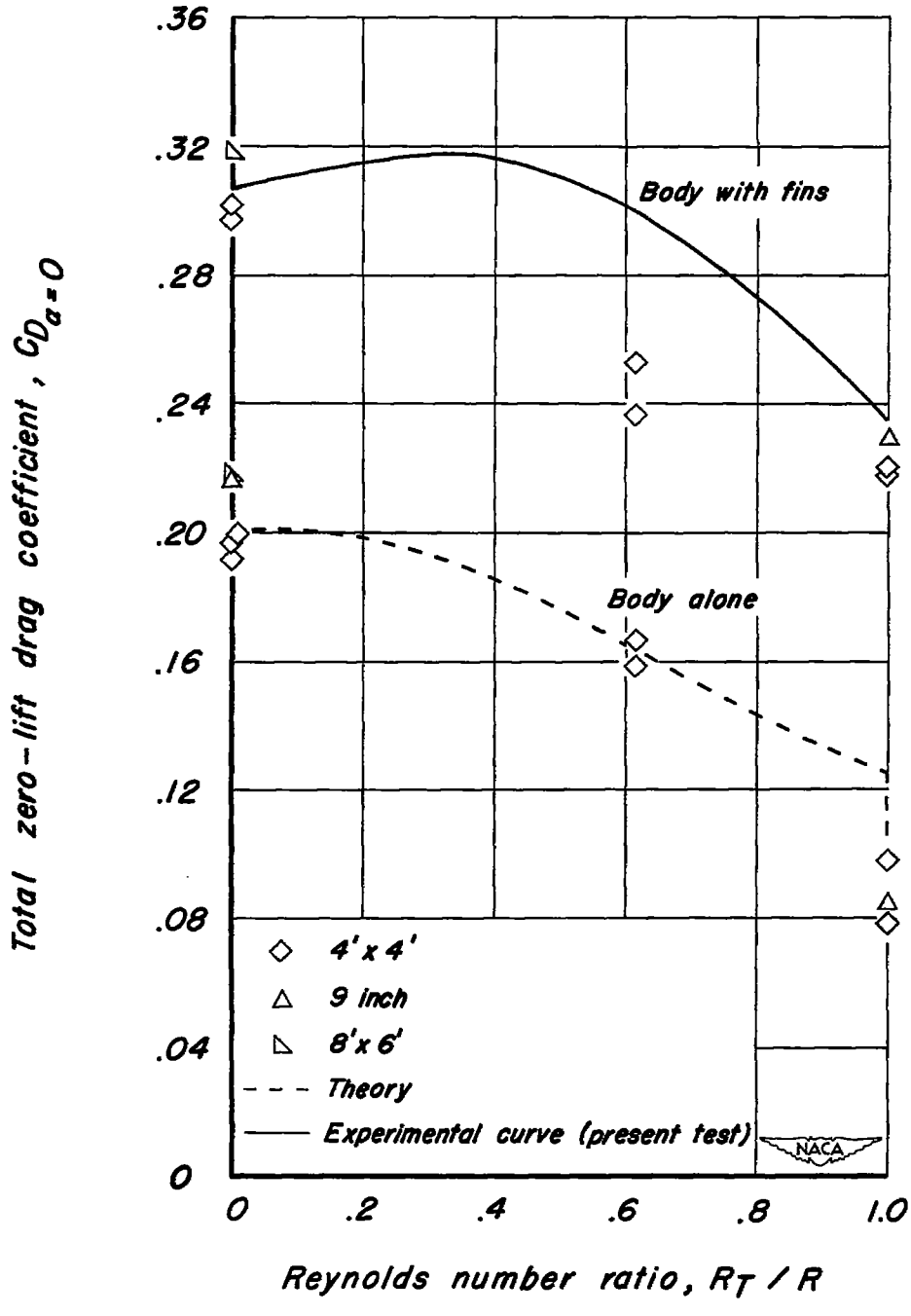

Figure 11.- Variation with transition location of the total zero-lift drag coefficient for other facilities ($M = 1.6$, $R = 3.0 \times 10^6$, $T_W = T_\infty$).